RNA sensor–induced type I IFN prevents diabetes caused by a β cell–tropic virus in mice

Stephen A. McCartney,[1] William Vermi,[2] Silvia Lonardi,[2] Cristina Rossini,[2] Karel Otero,[1] Boris Calderon,[1] Susan Gilfillan,[1] Michael S. Diamond,[1,3,4] Emil R. Unanue,[1] and Marco Colonna[1]

[1]Department of Pathology and Immunology, Washington University School of Medicine, St. Louis, Missouri, USA. [2]Department of Pathology I, University of Brescia, Spedali Civili 1, Brescia, Italy. [3]Department of Molecular Microbiology, and [4]Department of Medicine, Washington University School of Medicine, St. Louis, Missouri, USA.

Viral infections have been linked to the onset of type I diabetes (T1D), with viruses postulated to induce disease directly by causing β cell injury and subsequent release of autoantigens and indirectly via the host type I interferon (IFN-I) response triggered by the virus. Consistent with this, resistance to T1D is associated with polymorphisms that impair the function of melanoma differentiation associated gene-5 (*MDA5*), a sensor of viral RNA that elicits IFN-I responses. In animal models, triggering of another viral sensor, TLR3, has been implicated in diabetes. Here, we found that MDA5 and TLR3 are both required to prevent diabetes in mice infected with encephalomyocarditis virus strain D (EMCV-D), which has tropism for the insulin-producing β cells of the pancreas. Infection of *Tlr3*$^{-/-}$ mice caused diabetes due to impaired IFN-I responses and virus-induced β cell damage rather than T cell–mediated autoimmunity. Mice lacking just 1 copy of Mda5 developed transient hyperglycemia when infected with EMCV-D, whereas homozygous *Mda5*$^{-/-}$ mice developed severe cardiac pathology. TLR3 and MDA5 controlled EMCV-D infection and diabetes by acting in hematopoietic and stromal cells, respectively, inducing IFN-I responses at kinetically distinct time points. We therefore conclude that optimal functioning of viral sensors and prompt IFN-I responses are required to prevent diabetes when caused by a virus that infects and damages the β cells of the pancreas.

Introduction

Innate responses to viruses depend on pathogen recognition sensors that detect viral products and trigger the secretion of type I interferons (IFN-I), i.e., IFN-β and IFN-α (1–4). Two types of sensors detect double-stranded (ds) RNA generated during infection with RNA viruses: endosomal TLR-3 and cytoplasmic retinoic acid-inducible gene-I–like (RIG-I–like) receptors (RLR). TLR3 senses the dsRNAs that reach the endosomal compartment after phagocytosis of virally infected cells or apoptotic debris. RLRs include 2 IFN-inducible helicases, melanoma differentiation-associated gene 5 (MDA5) and RIG-I, which detect dsRNA intermediates that are generated in the cytoplasm during viral replication. MDA5 specializes in the detection of picornaviruses, whereas RIG-I senses many other RNA viruses (5). These viral specificities depend on the ability of MDA5 and RIG-I to recognize dsRNA molecules of different lengths, structures, and 5′ caps (6–9).

TLR3 transmits its intracellular signal through the adaptor protein Toll/IL-1 receptor domain–containing adaptor-inducing IFN-β (TRIF), which activates the transcription factor IFN regulatory factor-3 (IRF-3) and induces IFN-β production (1–4). RIG-I and MDA5 signal through another adaptor, IFN-β promoter stimulator-1 (IPS-1), which activates IRF-3 and IRF-7, inducing both IFN-β and IFN-α production. A third RLR, laboratory of genetics and physiology-2 (LGP2), detects dsRNA but lacks signaling domains and is thought to regulate MDA5 and RIG-I (10–12). IFN-I induces an antiviral state in uninfected cells and promote apoptosis of infected cells, limiting viral spread (13). Moreover, IFN-I has independent immunomodulatory effects and helps to orchestrate NK, T, and B cell responses, which facilitate viral clearance (13–15).

Type I diabetes (T1D) is an autoimmune disease that is primarily caused by selective destruction of islet β cells of the endocrine pancreas by autoreactive T cells (16, 17). Predisposing genetic factors, particularly MHC class II polymorphisms, play a predominant role in the pathogenesis of T1D. However, clinical (18–22) and experimental (23–25) studies have suggested that viral infections also may contribute to T1D, particularly infections by members of the enterovirus family of RNA viruses. These viruses may induce T1D by directly causing β cell damage and subsequent release of autoantigens that trigger autoreactive T cells (26–29). Paradoxically, the host IFN-I response can have detrimental effects when it activates preexisting autoreactive T cells that escaped thymic selection (30–33). Accordingly, a synthetic analog of viral dsRNA, poly(I:C), precipitates diabetes in mouse and rat models, acting in part through TLR3 (34–40). Consistent with this, genetic studies have recently shown that resistance to T1D is associated with polymorphisms in *MDA5* that diminish the IFN-I response to dsRNA (41–44). Collectively, these studies pose a conundrum: by eliciting IFN-I response, dsRNA sensors may limit the cytopathic effect of β cell–tropic viruses, but they can also precipitate T1D by promoting IFN-I–induced autoimmunity.

Herein, we evaluated the contributions of MDA5 and TLR3 to the host response to virus infection and development of diabetes using encephalomyocarditis virus strain D (EMCV-D). EMCV-D has preferential tropism for pancreatic β cells and can induce diabetes in selective mouse strains, such as DBA/2 (45, 46), as well

Authorship note: Stephen A. McCartney and William Vermi contributed equally to this work.

Conflict of interest: The authors have declared that no conflict of interest exists.

Citation for this article: *J Clin Invest.* 2011;121(4):1497–1507. doi:10.1172/JCI44005.

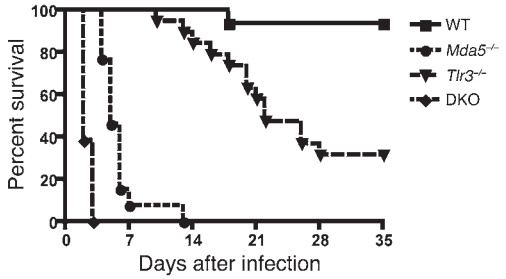

Figure 1
Both MDA5 and TLR3 protect from EMCV-D infection. WT, *Mda5*$^{-/-}$, *Tlr3*$^{-/-}$, and DKO mice were infected with 10^3 PFU of EMCV-D i.p. and monitored for survival (n = 20) in 2 independent experiments. WT mice survived infection, *Mda5*$^{-/-}$ mice succumbed on day 5, *Tlr3*$^{-/-}$ succumbed on day 22 with 30% surviving infection, and DKO mice succumbed on day 2.

as induce myocarditis. The relative roles of MDA5 and TLR3 in EMCV infection have been somewhat controversial. Initial studies indicated that MDA5 was essential for protection from lethal EMCV infection, whereas TLR3 was dispensable (47, 48); however, a subsequent study suggested that TLR3 provides protection from EMCV-induced myocarditis (49). We analyzed EMCV-D infection in *Mda5*$^{-/-}$, *Tlr3*$^{-/-}$, and *Mda5*$^{-/-}$*Tlr3*$^{-/-}$ double-knockout (DKO) mice and found that EMCV-D infection caused diabetes primarily in *Tlr3*$^{-/-}$ mice. Diabetes ensued due to β cell damage induced directly by the virus rather than autoimmune T cells; *Tlr3*$^{-/-}$ hematopoietic cells failed to induce an early IFN-β response that sufficiently limited β cell infection. EMCV-D infection also caused transient hyperglycemia in *Mda5*$^{+/-}$ mice, although overt diabetes was not observed in *Mda5*$^{-/-}$ mice, most likely because these mice developed severe cardiac pathology that caused premature death. Thus, our data suggest that MDA5 and TLR3 are not inherently diabetogenic, but rather can positively or negatively influence the sequence of pathological events that cumulate in diabetes. In autoimmune diabetes, inappropriate engagement of dsRNA sensors and excessive IFN-I release may trigger latent autoreactive T cells. In contrast, during infection with a β cell–tropic virus, attenuated activity of TLR3 and MDA5 results in blunted IFN-I response, uncontrolled viral replication, and direct β cell injury, which can result in diabetes if enough cells are destroyed.

Results

Both MDA5 and TLR3 contribute to survival from EMCV-D infection. To evaluate the roles of MDA5 and TLR3 in response to EMCV-D, we infected WT, *Mda5*$^{-/-}$, *Tlr3*$^{-/-}$, and *Mda5*$^{-/-}$ × *Tlr3*$^{-/-}$ (DKO) mice, all on a C57BL/6 background, with 1000 PFU via the i.p. route. Similar to previous reports, WT C57BL/6 mice survived EMCV-D infection, whereas *Mda5*$^{-/-}$ mice were highly susceptible and died on day 5 post infection (PI) (P < 0.001, n = 20; Figure 1). *Tlr3*$^{-/-}$ mice were also more susceptible to EMCV-D than WT mice (P < 0.001, n = 20), but less so than *Mda5*$^{-/-}$ mice, dying on average at day 22 PI, with some mice (~30%) surviving infection. Experiments with DKO mice confirmed the protective role of TLR3; DKO mice were more susceptible to EMCV-D than *Mda5*$^{-/-}$ mice, as they all died at day 2 PI (P < 0.001, n = 20; Figure 1) or at day 3 PI with an extremely low inoculating dose (1 PFU/mouse, data not shown). These results demonstrate that both MDA5 and TLR3 contribute to control of EMCV-D infection in vivo, with MDA5 having a predominant role.

Infection of Mda5$^{-/-}$ *and Tlr3*$^{-/-}$ *mice with EMCV-D causes different degrees of heart pathology*. Previous studies have implicated MDA5 (47) and TLR3 (49) in protection from EMCV-induced viral myocarditis using different strains of EMCV. To test the relative contributions of MDA5 and TLR3 to the protection of heart from EMCV-D, we measured levels of serum troponin, which reflects the extent of myocardial damage in WT, *Mda5*$^{-/-}$, *Tlr3*$^{-/-}$, and DKO mice after infection. Similar to previous findings (47), *Mda5*$^{-/-}$ mice had significantly elevated troponin levels by day 4 in comparison with WT mice (P < 0.01, n = 6) (Figure 2A). Correspondingly, the hearts of *Mda5*$^{-/-}$ mice showed higher EMCV-D titers (30-fold, P < 0.05), widespread immunoreactivity for EMCV-D antigen (EMCVpol), and early inflammatory infiltration (Figure 2, B–D). *Tlr3*$^{-/-}$ mice showed moderate infection in comparison with *Mda5*$^{-/-}$ mice. Troponin levels in *Tlr3*$^{-/-}$ mice were not significantly different from those in WT animals throughout the time course, although at day 7 a small subset of *Tlr3*$^{-/-}$ animals demonstrated increased troponin levels. Viral titers in the heart were only slightly higher in *Tlr3*$^{-/-}$ mice than in WT mice at all time points. EMCV antigen was limited to a few foci, and a modest infiltration of inflammatory cells was apparent at day 7, similarly to WT animals. The contribution of TLR3 to antiviral response against EMCV-D in the heart was also evident in the DKO mice. Earlier increase in troponin levels, higher levels of viral replication in the heart, and broader dissemination of EMCV antigen was observed when compared with *Mda5*$^{-/-}$ mice. Our experiments suggest that MDA5 has a dominant role in protecting against EMCV-D–induced myocarditis, with a subordinate contribution from TLR3.

TLR3 and MDA5 have nonredundant roles in the control of EMCV-D infection of pancreatic islets. It was previously shown that EMCV-D infects the pancreas, particularly the islet β cells, leading to the development of diabetes in susceptible mouse strains (e.g., DBA/2) (46). C57BL/6 mice, however, are normally resistant to EMCV-D–induced diabetes, and accordingly, WT mice sustained normal serum glucose levels after EMCV-D infection (Figure 3A). WT mice also showed no increase of the pancreatic enzymes amylase or lipase in the serum, suggesting a lack of significant damage of exocrine pancreas (Figure 3B). EMCV-D titers in the pancreas after infection with EMCV-D were increased at day 1 to 3 PI but cleared within a week (Figure 3C), and viral antigen and inflammatory infiltration were barely detectable (Figure 3, D and E). Similar to WT mice, *Tlr3*$^{-/-}$ mice showed minimal increases in amylase or lipase in the serum (Figure 3B). However, *Tlr3*$^{-/-}$ mice developed profound hyperglycemia by day 5 (Figure 3A) and by day 7 had lost almost all of their islet mass in the pancreas as assessed by staining with H&E (Figure 3E). *Tlr3*$^{-/-}$ mice supported higher viral titers in the pancreas at days 1 and 2 PI compared with WT and *Mda5*$^{-/-}$ mice, but normal clearance of EMCV-D by day 7 (Figure 3C). Moreover, EMCV antigen staining was concentrated mainly in the islets of *Tlr3*$^{-/-}$ mice (Figure 3D). Thus, TLR3 is essential for the protection of the endocrine pancreas from EMCV-D infection.

Mda5$^{-/-}$ mice showed no hyperglycemia and only a slight, nonsignificant increase in serum amylase and lipase at days 2 and 4 PI (Figure 3, A and B, and data not shown). Viral titers were similar to those of WT animals at day 1 PI, but markedly increased at day 2 PI (25-fold, P < 0.05) and remained elevated (160-fold, P < 0.01) until the mice died (Figure 3C). Consistent with this, *Mda5*$^{-/-}$ mice showed disseminated antigen staining in both the endocrine and exocrine pancreas as well as marked inflammatory infiltration

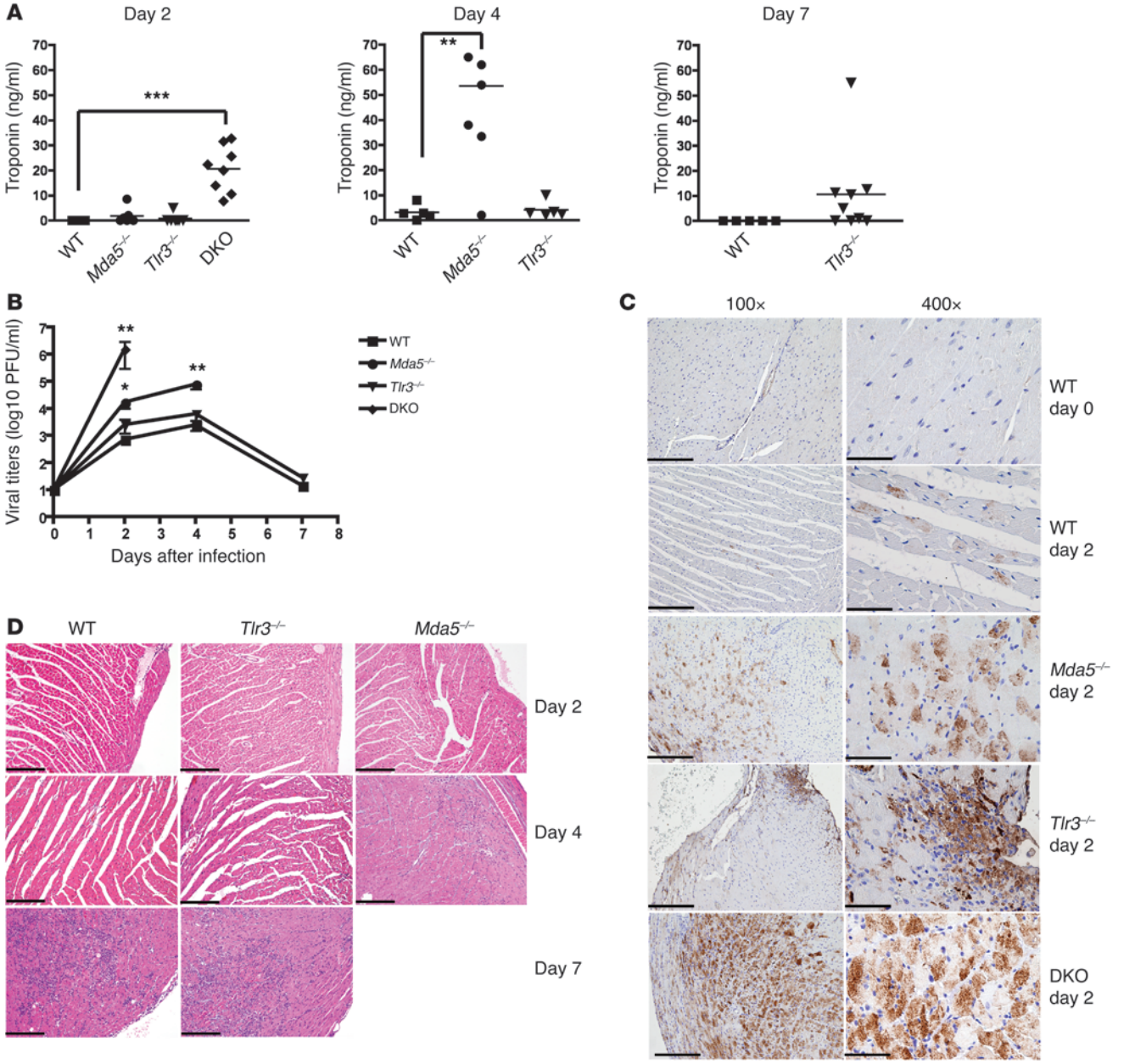

Figure 2

MDA5 controls EMCV-D infection in the heart. WT and KO mice were infected with 10^3 PFU of EMCV-D. Serum and heart ($n \geq 6$ per time point, 3 independent experiments) were harvested at days 2, 4, and 7 from surviving mice and were evaluated for (**A**) troponin levels by ELISA and (**B**) virus titer by plaque assay or fixed in formalin and paraffin embedded for histology. Tissue sections were stained for EMCVpol antigen by immunohistochemistry (**C**) (left column: original magnification, ×100 magnification; scale bars: 200 microns; right column: original magnification, ×400; scale bars: 50 micron) or stained by H&E and evaluated for pathology (**D**) (original magnification, ×100; scale bar: 200 micron). In **C**, strong and diffuse EMCVpol reactivity is particularly evident in the myocardium of *Mda5*$^{-/-}$ and DKO; in contrast, heart from WT and *Tlr3*$^{-/-}$ animals showed only mild (WT) or focal (*Tlr3*$^{-/-}$) staining, which is shown in detail in the right panel. In **D**, areas of myocarditis are observed in WT and *Tlr3*$^{-/-}$ on day 7 PI as well as in *Mda5*$^{-/-}$ day 4 PI; only mild inflammation is observed in *Tlr3*$^{-/-}$ day 4 PI. Statistical significance was calculated by 2-tailed Student's *t* test and is indicated as follows: $^*P < 0.05$; $^{**}P < 0.01$; $^{***}P < 0.001$.

of the islets (Figure 3, D and E). Given these histopathological changes, the finding that *Mda5*$^{-/-}$ mice did not develop hyperglycemia was somewhat surprising. We hypothesized that the severe cardiac pathology in these animals caused early death so that the diabetes never developed. To test this, we used EMCV-D to infect *Mda5*$^{+/-}$ mice, which have a single WT allele of MDA5. The *Mda5*$^{+/-}$ mice developed transient hyperglycemia beginning on day 5 that resolved by day 12, yet had no survival defect compared with WT animals (Figure 3F and data not shown) in response to EMCV-D infection. Correspondingly, *Mda5*$^{+/-}$ mice had slightly increased viral titers in the pancreas at day 4 compared with WT animals (Figure 3G). Furthermore, in contrast to animals on the C57BL/6

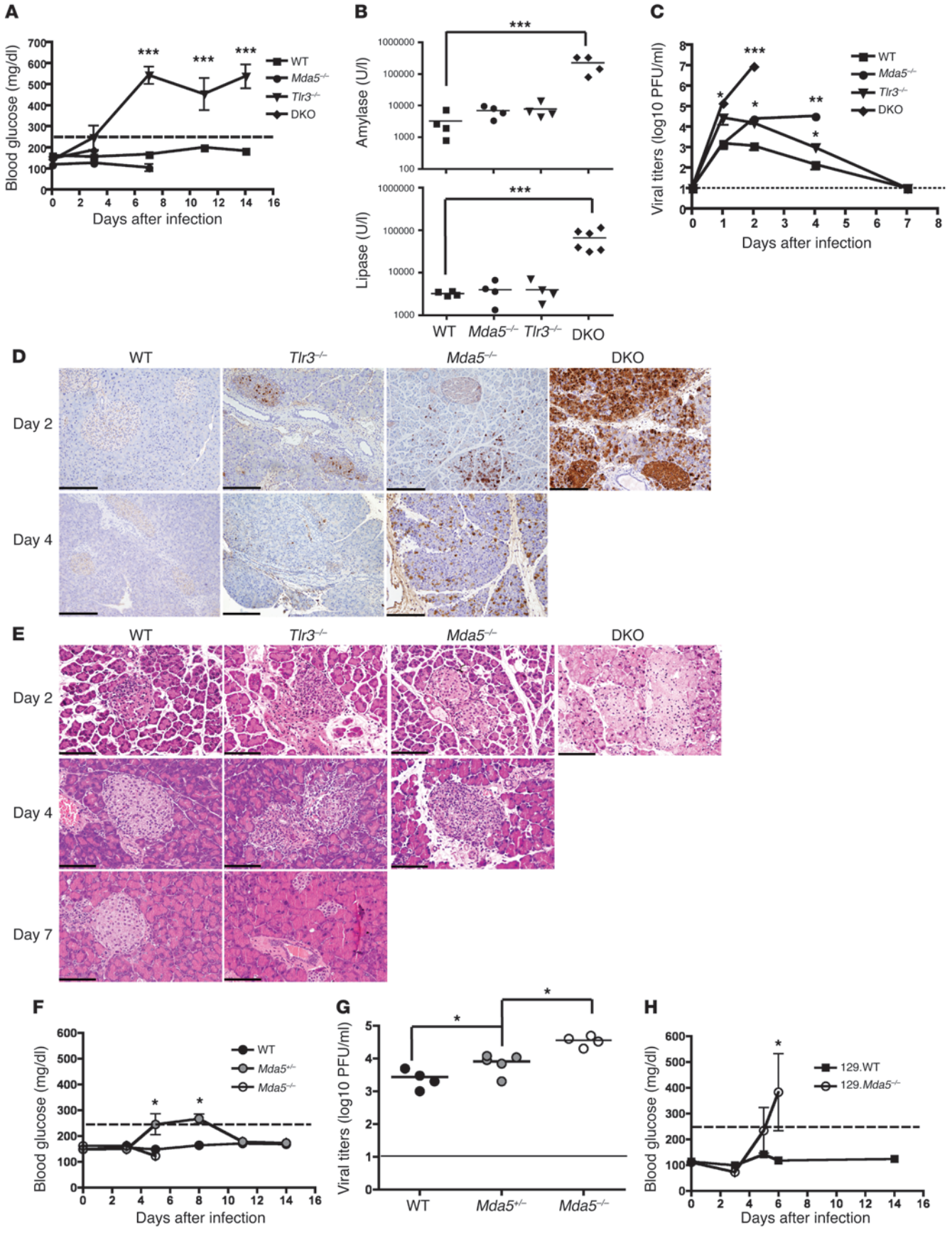
A
Blood glucose (mg/dl)
Days after infection
WT
Mda5−/−
Tlr3−/−
DKO
***
B
Amylase (U/l)
Lipase (U/l)
WT
Mda5−/−
Tlr3−/−
DKO
C
Viral titers (log10 PFU/ml)
Days after infection
D
WT
Tlr3−/−
Mda5−/−
DKO
Day 2
Day 4
E
Day 2
Day 4
Day 7
F
Blood glucose (mg/dl)
Days after infection
Mda5+/−
G
Viral titers (log10 PFU/ml)
H
129.WT
129.Mda5−/−

Figure 3
TLR3 and MDA5 protect pancreatic islets from EMCV-D infection. WT and KO mice were infected with 10^3 PFU EMCV-D. Serum samples were evaluated for (**A**) blood glucose ($n \geq 8$) or (**B**) amylase and lipase ($n \geq 4$) at the indicated times after infection in 2 independent experiments. The pancreas was harvested at the indicated times and viral titers were determined by plaque assay (**C**) ($n = 6$ per time point, 3 independent experiments) or fixed in formalin and paraffin embedded for histology. Tissue sections were stained using anti-EMCVpol (**D**) by immunohistochemistry ($n > 3$) to visualize virus infiltration (original magnification, ×100; scale bars: 200 micron) or by H&E and evaluated for pathology (**E**) (original magnification, ×200; scale bars: 100 micron). To further examine the role of MDA5 for protection in the pancreas, *Mda5*$^{+/-}$ animals on the C57BL/6 background were infected with EMCV-D in parallel with WT and *Mda5*$^{-/-}$ animals and were evaluated for blood glucose (**F**) and pancreatic viral titers (**G**) ($n = 5$). In addition, *Mda5*$^{-/-}$ animals on the 129/SvJ background were evaluated for hyperglycemia (**H**) ($n = 12$) after infection with EMCV-D. Statistical significance was calculated by 2-tailed Student's *t* test and is indicated as follows: *$P < 0.05$; **$P < 0.01$; ***$P < 0.001$.

background, *Mda5*$^{-/-}$ mice on the 129/SvJ genetic background developed hyperglycemia after EMCV-D infection before death (Figure 3H). Collectively, these data suggest that MDA5 activity is necessary for protection of β cells from viral infection and that both TLR3 and MDA5 have nonredundant roles in preventing damage of pancreatic islets.

EMCV-D infection spreads to the exocrine pancreas in the absence of both TLR3 and MDA5. While EMCV-D infection of *Mda5*$^{-/-}$ or *Tlr3*$^{-/-}$ mice did not cause overt pancreatitis, examination of DKO mice demonstrated a significant increase of serum levels of amylase (70-fold, $P < 0.001$) and lipase (25-fold, $P < 0.001$) compared with WT mice (Figure 3B). This was associated with a large increase in viral titers and extensive destruction of pancreatic architecture in both the exocrine and endocrine tissue on day 2 (Figure 3, C–E). Thus, virus-induced pancreatitis is likely the primary cause of death of DKO mice at day 2 PI. Although high-grade infection of the islets was observed, DKO mice did not develop hyperglycemia, possibly due to the associated pancreatitis and rapid death. These results indicate that MDA5 and TLR3 are sufficient to prevent EMCV-D spreading in the exocrine pancreas, such that only an absence of both sensors results in significant infection causing overt and destructive pancreatitis.

TLR3 and MDA5 act in different cell compartments. To gain more insight into the pathogenesis of EMCV-D–induced diabetes, we assessed how cell-specific expression of TLR3 and MDA5 affected control of infection in the pancreas. We generated reciprocal BM chimeras between WT and *Mda5*$^{-/-}$ or WT and *Tlr3*$^{-/-}$ mice and measured survival and blood glucose levels after EMCV-D infection. Survival analysis showed that chimeras containing *Mda5*$^{-/-}$ hematopoietic cells and WT stroma (*Mda5*$^{-/-}$→WT) were resistant to EMCV-D infection, whereas WT→*Mda5*$^{-/-}$ chimeras were vulnerable to infection (100% lethality, $P < 0.001$, $n = 10$) analogous to *Mda5*$^{-/-}$ mice. *Tlr3*$^{-/-}$→WT chimeras were more sensitive (30% lethality, $P < 0.05$, $n = 12$) to EMCV-D infection than WT→*Tlr3*$^{-/-}$ chimeras, although less so than WT→*Mda5*$^{-/-}$ chimeras (Figure 4A). Thus, the overall resistance to EMCV-D infection is primarily dependent on MDA5 function in radio-resistant nonhematopoietic cells, whereas TLR3 contributes to defense in part because of its effect in hematopoietic cells. The analysis of blood glucose after EMCV-D infection revealed that *Tlr3*$^{-/-}$→WT chimeras developed diabetes, whereas WT→*Tlr3*$^{-/-}$ chimeras as well as *Mda5*$^{-/-}$→WT were protected (Figure 4B). Thus, TLR3 protects β cells from EMCV-D infection through its effects in the radio-sensitive hematopoietic compartment. Most likely, MDA5 prevents EMCV-D infection of β cells by acting in the radio-resistant nonhematopoietic compartment, although this hypothesis could not be directly tested, because WT→*Mda5*$^{-/-}$ chimeras died rapidly at days 5–6 before they could develop diabetes.

We then asked which MDA5$^+$ stromal and TLR3$^+$ hematopoietic cells prevent the development of diabetes. Immunohistochemical analysis showed that MDA5 is broadly induced in both islets and exocrine pancreas during viral infection, suggesting that MDA5 may act locally (Figure 4C). In contrast, TLR3 was expressed in few myeloid cells in the islets as well as in duct epithelial cells, vascular endothelial cells, and interstitial cells (Figure 4D). Notably, the myeloid cells in the islets had dendritic morphology, suggesting that they could be a DC subset, although relatively few expressed CD11c (Figure 5A). To determine whether DCs contribute to protection, we infected CD11c-DTR transgenic mice, which allow selective depletion of CD11c$^+$ cells after administration of diphtheria toxin (DT) (50). Mice that were treated with DT on day –1 prior to EMCV-D infection developed hyperglycemia on day 4 compared with PBS-treated animals, which did not develop diabetes (Figure 5B). Additionally, DT-treated mice suffered uniform lethality by day 5 PI (Figure 5C), had increased viral titers in the pancreas, spleen, and heart (Figure 5D), and showed reduced levels of systemic IFN-I compared with controls (Figure 5E). Immunohistochemistry showed that DT treatment resulted in depletion of the few CD11c$^+$ cells in the pancreas as well as massive depletion of CD11c$^+$ cells in the marginal and periarteriolar zones of the spleen (Figure 5F). Because most of these CD11c$^+$ splenocytes express TLR3 (Figure 5G and refs. 51, 52), TLR3 may act locally in islet DCs and also in DCs of the spleen and other organs that control the systemic level of EMCV infection.

In addition to DCs, TLR3 is also known to be expressed on macrophages. To assess the potential involvement of these cells in preventing virus-induced diabetes, we infected WT mice that had been injected with clodronate-containing liposomes to deplete macrophages (53). Macrophage depletion did not cause hyperglycemia, but markedly increased mortality of WT mice following EMCV-D infection (Supplemental Figure 1; supplemental material available online with this article; doi:10.1172/JCI44005DS1), probably reflecting a role of splenic or other macrophage populations in controlling viral infection, as has been observed for other viruses (54). Thus, TLR3-mediated control of EMCV-D infection and diabetes may involve DC and possibly other TLR3$^+$ myeloid cells that reside in the islets or infiltrate the islets during infection. Additionally, TLR3 may act in systemic DCs and macrophages, controlling global viral titers and the course of infection.

The IFN-I responses to EMCV-D induced by MDA5 and TLR3 are distinct in terms of amplitude and kinetics. The nonredundant roles of TLR3 and MDA5 in controlling EMCV-D infection of β cells prompted us to evaluate their relative impact on IFN-I responses to EMCV-D. We noticed that *Tlr3*$^{-/-}$ mice had higher viral titers in the pancreas compared with either WT or *Mda5*$^{-/-}$ mice at early time points PI (see Figure 3C), whereas *Mda5*$^{-/-}$ mice developed higher viral titers than either WT or *Tlr3*$^{-/-}$ mice at later time points (see Figure 3C). Based on this, we hypothesized that TLR3 and MDA5 prevent EMCV-D–induced diabetes by induc-

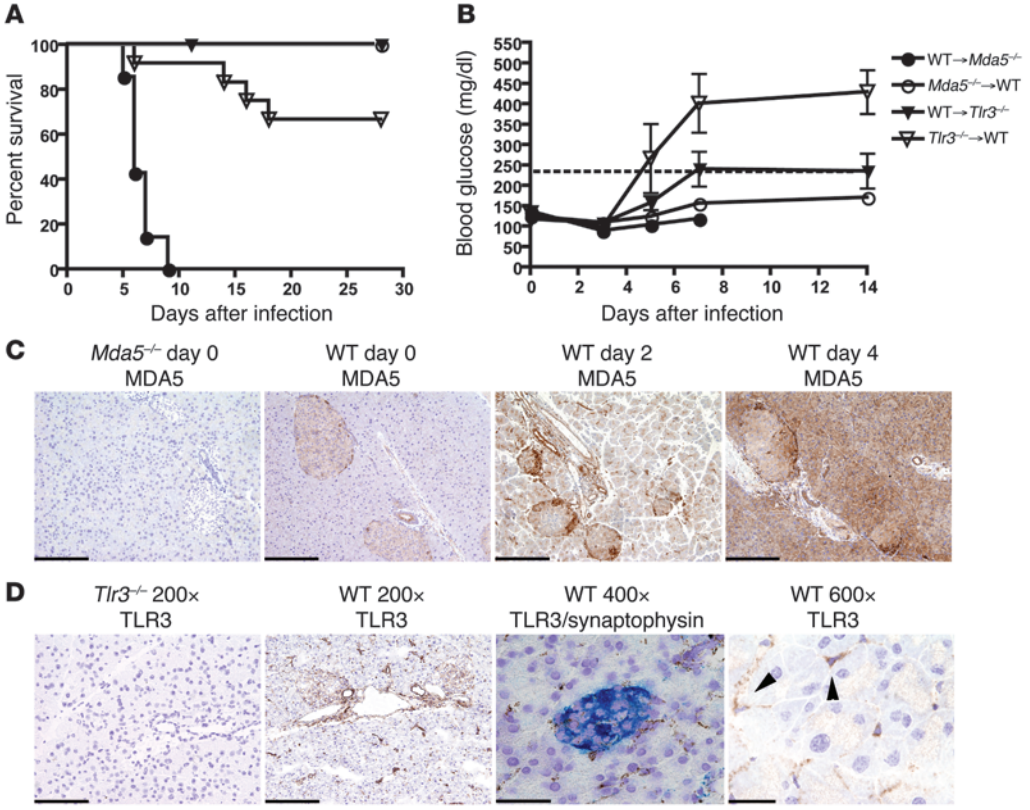

Figure 4

Stromal MDA5 and hematopoietic cell TLR3 protect against EMCV-D infection. (**A** and **B**) BM chimeras were generated between WT and *Mda5*$^{-/-}$ (n = 10 each) and WT and *Tlr3*$^{-/-}$ animals (n = 12 each) in 2 independent experiments. Chimeras were infected with 10^3 PFU of EMCV-D and evaluated for (**A**) survival and (**B**) blood glucose. *Mda5*$^{-/-}$→WT and WT→*Tlr3*$^{-/-}$ chimeras survived infection, WT→*Mda5*$^{-/-}$ chimeras succumbed on day 6, and *Tlr3*$^{-/-}$→WT chimeras succumbed on day 14 with 67% surviving infection. (**C**) MDA5 expression in the pancreas (original magnification, ×200; scale bars: 100 micron). Fixed tissue sections were made from *Mda5*$^{-/-}$ and WT pancreas on days 0, 2, and 4 after EMCV infection and stained with anti-MDA5 (n = 3). MDA5 is expressed in islets before infection and induced in both islets and exocrine pancreas after infection. (**D**) TLR3 expression in the pancreas. Frozen tissue sections were made from WT and *Tlr3*$^{-/-}$ pancreas from uninfected animals (first, second, and fourth panels) or from WT pancreas 12 hours after EMCV infection (third panel). Sections were stained with anti-TLR3 (brown) or costained with anti-TLR3 (brown) and synaptophysin (blue) to visualize expression in the islets (third panel) and are shown at different magnifications as indicated (original magnification, ×200, scale bars: 100 micron; original magnification, ×400, scale bars: 50 micron; original magnification, ×600, scale bars: 33 micron) (n = 3). TLR3 expression is found in the islets as well as in duct epithelial cells, vascular endothelial cells and interstitial stromal cells (arrowheads indicate TLR3$^+$ interstitial cells).

ing IFN-I at different time points after infection. To evaluate this, we measured IFN-I in the serum of infected mice using a sensitive and validated bioassay. Notably, IFN-I levels were reduced (10-fold, $P < 0.01$) in *Mda5*$^{-/-}$ compared with WT mice 24 hours after infection; the residual systemic IFN-I response in *Mda5*$^{-/-}$ mice was dependent on TLR3, as no IFN-I was detected in the serum of DKO mice (Figure 6A). Thus, the quantitative impact of MDA5 and TLR3 on the accumulation of IFN-I in serum is distinct, with MDA5 responsible for the majority of it. MDA5 and TLR3 also contributed differently to the kinetics of the IFN-I response. IFN-I was detected as early as 15 hours after EMCV-D infection in the serum of WT and *Mda5*$^{-/-}$ mice, whereas it was detected only later in *Tlr3*$^{-/-}$ mice. We conclude that TLR3 and MDA5 induce IFN-I responses with distinct amplitude and kinetics, both of which are essential for protecting the endocrine pancreas from EMCV-D infection.

The TLR3–IRF3–IFN-β axis in hematopoietic cells prevents EMCV-D–induced diabetes. TLR3-mediated signals activate the transcription factor IRF-3, which binds the IFN-β promoter and induces IFN-β production and secretion (55). If the early IFN-β production induced by TLR3 is necessary to prevent EMCV-D–induced diabetes, mice deficient in IRF-3 or IFN-β also should develop diabetes after EMCV-D infection. To test this, we infected *Irf3*$^{-/-}$ and *Ifnb*$^{-/-}$ mice with EMCV-D and measured blood glucose levels. Notably, both *Irf3*$^{-/-}$ and *Ifnb*$^{-/-}$ mice developed hyperglycemia after infection (Figure 6B). However, both strains of deficient mice were more susceptible to EMCV-D and died earlier than did the *Tlr3*$^{-/-}$ mice (Figure 6C), most likely because a global defect in either IRF-3 or IFN-β impairs additional antiviral pathways than those triggered by TLR3 alone. Because TLR3 must be expressed in the hematopoietic compartment to protect from EMCV-D–induced diabetes, we hypothesized that a defect of IRF-3 and IFN-β limited to the hematopoietic compartment should be sufficient to induce diabetes. To test this, we created *Irf3*$^{-/-}$→WT and *Ifnb*$^{-/-}$→WT BM chimeras, which were then infected with EMCV-D. Both chimeras developed hyperglyce-

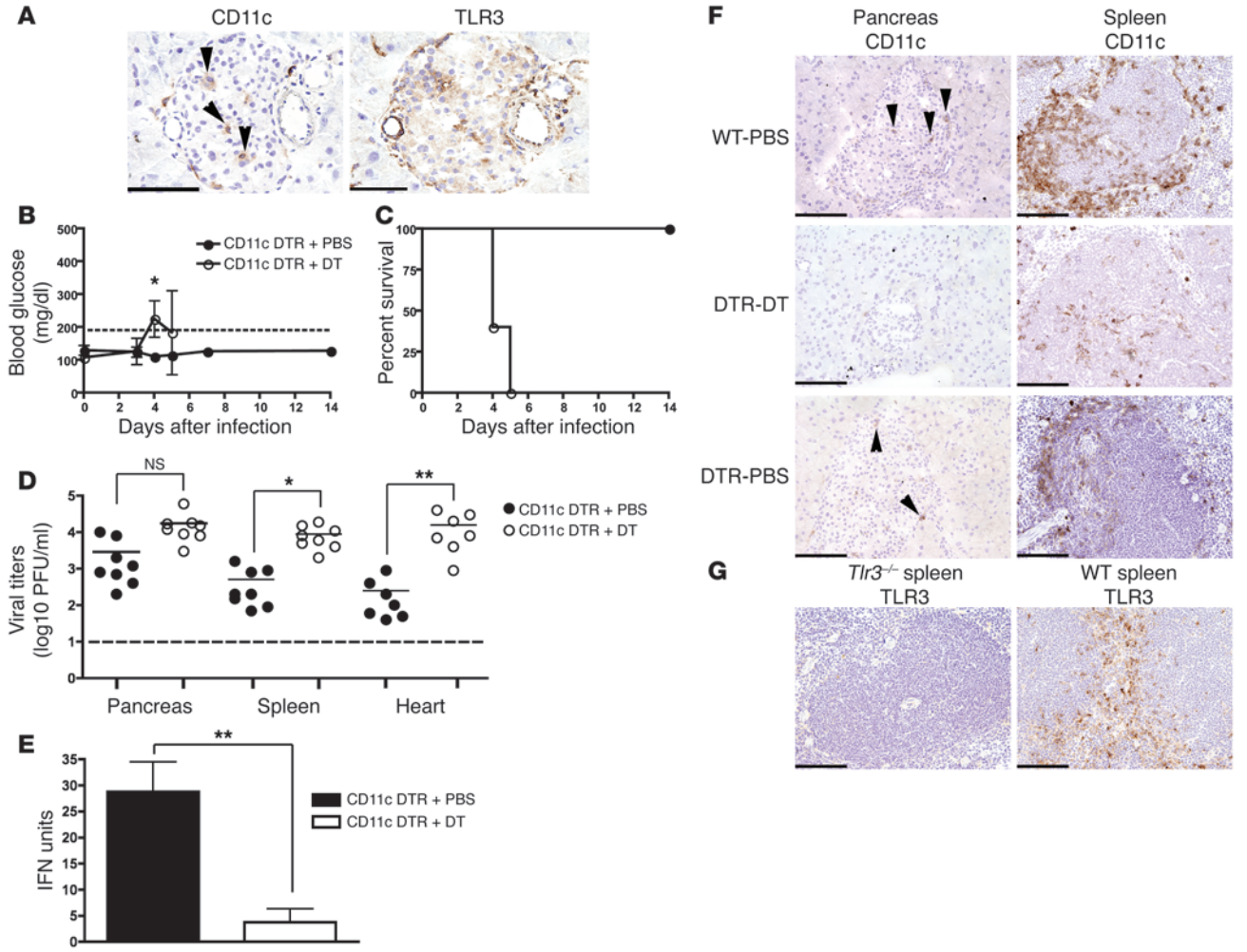

Figure 5

CD11c+ DC control EMCV-D infection and development of diabetes. (**A**) Identification of CD11c+ DCs in the islets. Serial frozen sections were made from the pancreas of uninfected WT animals and stained with anti-CD11c (left panel) and anti-TLR3 (right panel) (original magnification, ×400; scale bar 50 micron) (n = 3). Arrowheads indicate CD11c+ cells that are also TLR3+. (**B**–**E**) CD11c+ DC are required for protection from EMCV-D–induced diabetes. CD11c-DTR mice were treated with PBS (n = 8) or DT (n = 8), then monitored for (**B**) blood glucose, (**C**) survival, (**D**) organ viral titers in the pancreas, heart, and spleen, and (**E**) serum IFN-I after EMCV-D infection. (**F**) Frozen sections were prepared from WT and CD11c-DTR PBS and DT-treated mice 48 hours after treatment. Immunohistochemical analysis of CD11c+ cells in the pancreas and spleens of these animals revealed depletion primarily in the spleen after DT treatment (original magnification, ×200; scale bars: 100 micron) (n = 3). Arrowheads indicate CD11c+ cells in the pancreas. (**G**) Frozen sections of spleens from WT and *Tlr3*$^{-/-}$ mice were used to perform immunohistochemical evaluation of TLR3 expression in the marginal and periarteriolar zones of the spleen (original magnification, ×200, scale bars: 100 micron) (n = 3). Statistical significance was calculated by 2-tailed Student's t test and is indicated as follows: *P < 0.05; **P < 0.01.

mia after infection and had a mild survival defect analogous to the *Tlr3*$^{-/-}$→WT BM chimeras (Figure 6, D and E). These data strongly support the hypothesis that early IFN-β production by hematopoietic cells through a TLR3–IRF-3 signaling axis is critical for protection from EMCV-D–induced diabetes.

EMCV-D infection in Tlr3$^{-/-}$ *mice is associated with* β *cell apoptosis and myeloid infiltrate*. T1D is commonly caused by autoimmune destruction of pancreatic islets by autoreactive T cells. EMCV-D–induced diabetes in *Tlr3*$^{-/-}$ mice, however, did not appear to cause a significant T cell infiltration of pancreatic islets after infection (data not shown), making the involvement of an autoimmune mechanism less likely. At early time points, pancreatic islets of *Tlr3*$^{-/-}$ mice showed prominent staining for viral antigen compared with WT mice confirming the viral titer data (Figure 3D). Additionally, islets from infected *Tlr3*$^{-/-}$ mice demonstrated marked apoptosis and a robust infiltrate of myeloid cells as assessed by staining for activated caspase-3 and the myeloid marker Iba-1, respectively (Figure 7, A and B). These myeloid cells may be macrophages, which phagocytose virally infected apoptotic cells. In comparison, WT mice showed limited accumulation of myeloid cells around but not within the pancreatic islets. The extensive viral replication and apoptosis in the pancreatic islets of *Tlr3*$^{-/-}$ mice suggest that in this model diabetes is due to failure to control local EMCV-D infection. This conclusion is consistent with previous reports showing that EMCV-induced diabetes in susceptible mouse strains is due to direct β cell damage (25). Analogously, the transient hyperglycemia observed in *Mda5*$^{+/-}$ mice also likely is due to suboptimal control of EMCV-D infection, resulting in limited damage of β cells.

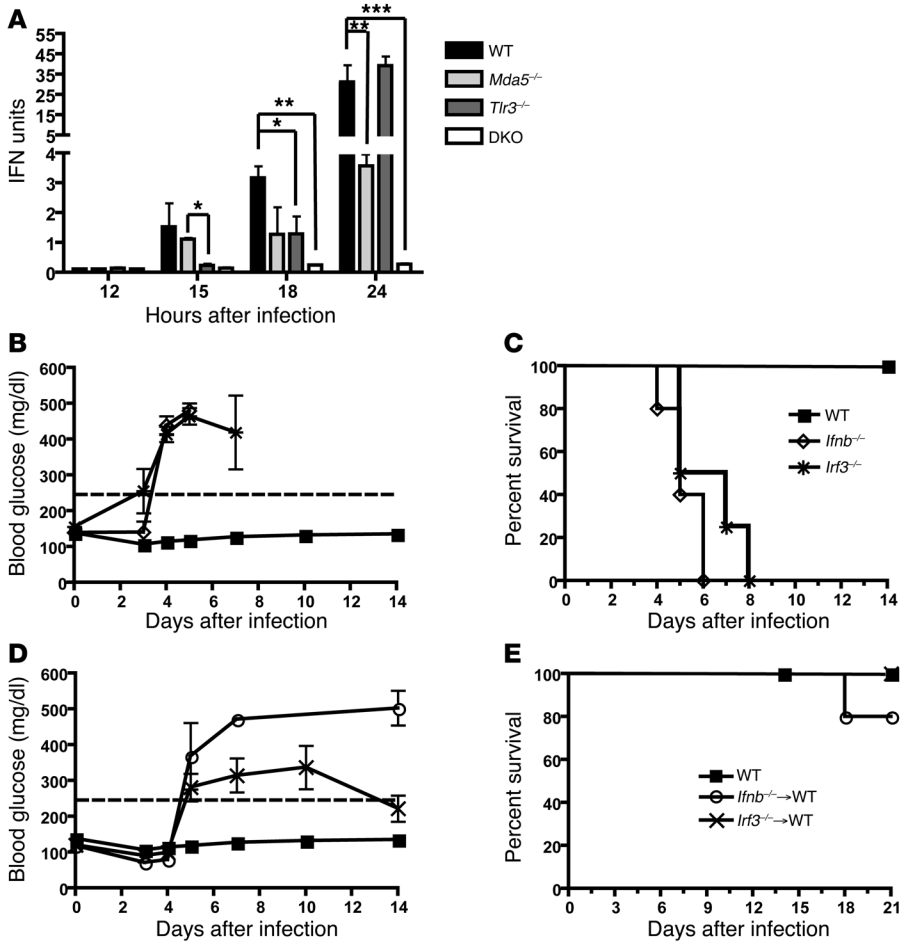

Figure 6
MDA5 and TLR3 induce type I IFN responses that are distinct in timing and magnitude. (**A**) Serum samples from WT, *Mda5*$^{-/-}$, *Tlr3*$^{-/-}$, and DKO mice were harvested at specified time points after EMCV-D infection and evaluated for type I IFN production by bioassay (n = 6 samples per time point performed in duplicate; results from 3 independent experiments). *Irf3*$^{-/-}$ (n = 8; 2 independent experiments) and *Ifnb*$^{-/-}$ (n = 6) mice were infected with EMCV-D and monitored for (**B**) blood glucose levels and (**C**) survival. BM chimeras with *Irf3*$^{-/-}$ or *Ifnb*$^{-/-}$ BM into WT hosts (n = 6 for each) were infected with EMCV-D and monitored for (**D**) blood glucose and (**E**) survival. Statistical significance was calculated by 2-tailed Student's t test and is indicated as follows: *P < 0.05; **P < 0.01; ***P < 0.001.

Discussion

This study demonstrates that TLR3 is an essential component in the defense against virus-induced diabetes in the EMCV-D model. MDA5 also protects β cells from viral insult, as lack of 1 allele is sufficient to cause transient hyperglycemia. The in vivo role of TLR3 in host defense against EMCV-D has been controversial. Although initial studies did not detect any role of TLR3 in the defense of EMCV (47), more recent experiments have revealed that TLR3 contributes to the antiviral response against EMCV (49). Here, we demonstrated that TLR3 protects against EMCV-D infection, but its impact varies in different organs. TLR3 plays a subordinate role in comparison with MDA5 in controlling cardiac infection and disease by EMCV-D. However, TLR3 is essential and nonredundant in the defense of pancreatic β cells and also contributes with MDA5 in limiting EMCV-D spread to the exocrine pancreas.

TLR3 and MDA5 differed in the magnitude and timing of the IFN-I responses that they induced. We confirmed that MDA5 induces the bulk of IFN-I systemic response after EMCV-D infection. The reduced magnitude of IFN-I responses in the *Mda5*$^{-/-}$ mice explains the survival defect, whereas *Tlr3*$^{-/-}$ mice showed a comparatively mild defect. Nonetheless, we found that TLR3 mediates the systemic IFN-I response at very early time points. The delayed kinetics of the IFN-I response in *Tlr3*$^{-/-}$ mice is sufficient to impair the control of viral infection in endocrine pancreas, resulting in diabetes. Finally, TLR3 and MDA5 acted in different cellular compartments to control EMCV-D infection. BM reconstitution studies demonstrated that MDA5 and TLR3 act preferentially in stromal and hematopoietic compartments, respectively, for the control of EMCV infection. MDA5 may directly act in the islets, where it is broadly expressed and is further induced by IFN-I. TLR3 may act in myeloid cells that are present in the islets as well as in DCs of the spleen and other organs that control global viral titers.

For decades, clinical studies and experimental models have implicated viral infections and host type I IFN response in the pathogenesis of T1D (30, 33). It has been proposed that viruses and dsRNA may trigger diabetes through the sustained production of IFN-I, which promotes autoimmune T cell responses (30). Consistent with this hypothesis, genetic studies in humans have shown that rare *MDA5* alleles, which are defective for IFN-I production, correlate with protection from developing T1D (41–44). In apparent contrast with these studies, we found that impaired detection of EMCV-D and IFN-I response in mice that lack TLR3 in hematopoietic cells results in diabetes. In this instance, however, diabetes is due to virus-induced β cell damage rather than T cell–mediated autoimmunity. As mice that were heterozygous for the WT MDA5 allele also developed EMCV-D–induced hyperglycemia, MDA5 likely also prevents virus-induced diabetes, although this conclusion could not be formally demonstrated because a complete absence of MDA5 resulted in rapid EMCV-D–induced mortality prior to the development of diabetes. We propose that the responses induced by TLR3 and MDA5 are not

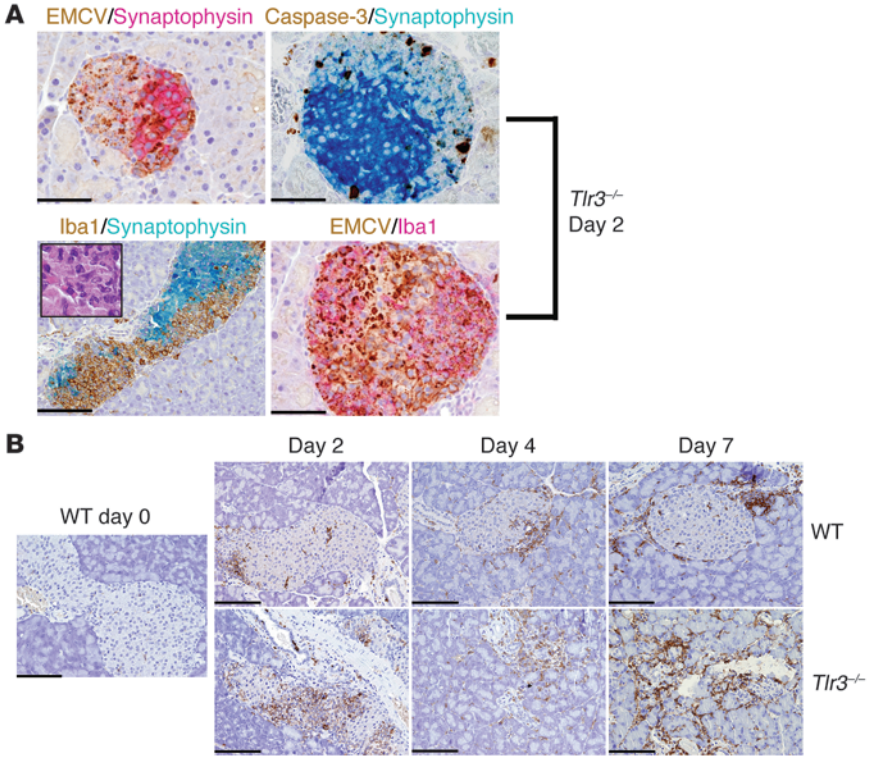

Figure 7
EMCV-D–induced diabetes in *Tlr3*$^{-/-}$ mice is characterized by islet infection, apoptosis, and myeloid cell infiltrate. Pancreas tissue samples from WT or *Tlr3*$^{-/-}$ mice were harvested at days 0, 2, 4, or 7 PI as indicated, fixed in formalin, and paraffin embedded. (**A**) Sections were costained with anti-EMCVpol (brown) and anti-synaptophysin (red) (top left panel); active caspase-3 (brown) and anti-synaptophysin (blue) (top right panel); anti–Iba-1 (brown) and anti-synaptophysin (blue) with H&E-stained insert (bottom left panel); or anti-EMCVpol (brown) and anti–Iba-1 (red) (bottom right panel) (left panels: original magnification, ×200, scale bars: 100 micron, right panels: original magnification, ×400, scale bars: 50 micron). By morphology, Iba-1$^+$ cells correspond to large cells with irregular nuclei resembling macrophages (**A**, bottom left panel insert). As demonstrated by double immunohistochemistry, these islets contain numerous apoptotic cells and Iba1$^+$ cells that react with antibodies against EMCVpol. (**B**) To visualize myeloid cell infiltrates, sections from WT and *Tlr3*$^{-/-}$ pancreas were stained with anti–Iba-1 (original magnification, ×200; scale bars: 100 micron). In WT pancreas, Iba-1$^+$ cells are found at the periphery of the islets, whereas In *Tlr3*$^{-/-}$, Iba-1$^+$ cells infiltrate the islet.

inherently diabetogenic and instead depend on the pathogenesis sequence that causes diabetes. In autoimmune T1D, dsRNA sensors may be inappropriately stimulated by endogenous nucleic acids generated by cell apoptosis or necrosis or by viral infections that do not target β cells. This may lead to excessive IFN-I that triggers latent autoreactive T cells. In contrast, during infection with β cell–tropic viruses, attenuated activity of dsRNA sensors, particularly TLR3 in hematopoietic cells, may lead to blunted IFN-I response, uncontrolled virus replication, and diabetes. Interestingly, the analysis of pancreatic tissue from recent-onset diabetic patients demonstrated distinct histological patterns that reflected either autoimmune or viral pathogenesis (56). While normal- or hyperfunctional polymorphisms in human *MDA5* predispose to autoimmune T1D, hypofunctional polymorphisms in *TLR3* (and possibly *MDA5*) may predispose to susceptibility to virus-induced diabetes, provided that the triggering pathogens are present in the environment (57).

Methods

Mice and infections. *Mda5*$^{-/-}$ and *Mda5*$^{+/-}$ (48), *Tlr3*$^{-/-}$ (51), DKO (51), CD11c-DTR (58), *Irf3*$^{-/-}$ (59), and *Ifnb*$^{-/-}$ (60) mice have been described previously. All mice were backcrossed to the C57BL/6 background as determined by speed congenics (Washington University Rheumatic Diseases core facility). *Mda5*$^{-/-}$ mice on the 129/SvJ genetic background have been described (48). Age-matched control mice were purchased commercially (Jackson Laboratories). All mice used in these experiments were male because male mice are more susceptible to EMCV-D–induced diabetes (ref. 45 and data not shown). EMCV-D was obtained from John Corbett (University of Alabama, Birmingham, Alabama, USA) and was passaged in L929 cells. Infections were performed at 1000 PFU per mouse by i.p. injection. All animal studies were approved by the Washington University Animal Care Committee.

BM chimera generation. Recipient mice were γ-irradiated with 10 Gy. After an overnight rest, mice were reconstituted with 5×10^6 BM cells per mouse that had been harvested from the femurs and tibias of age-matched donors. After 6 weeks, chimeras were used for infections.

Virus titers. Organs from infected animals were frozen at –80°C immediately after harvest. Subsequently, organs were suspended in 1 ml DMEM (Invitrogen) and homogenized by bead-beating with 1.0 mm beads (BioSpec Products). Organ homogenates were diluted 1:10 in DMEM and tested for viral titers in a plaque assay. L929 cells were seeded in 6-well plates and infected with 10-fold dilutions of tissue homogenate in duplicate. After 1-hour incubation, media was removed and wells were overlaid with complete DMEM media (DMEM with 10% FCS [HyClone], 10 mM HEPES [Invitrogen], and 50 units/ml penicillin/streptomycin [Invitrogen] containing 1.5% SeaPlaque agarose [Cambridge Biosciences]). After 48 hours, a second overlay was added containing 1.5% SeaKem agarose (Cambridge Biosciences) and 0.01% neutral red (Sigma-Aldrich) in complete DMEM media. After 8 hours, plaques were then visualized.

Blood/serum measurements. Blood was collected at specified time points after infection and centrifuged in serum separator tubes (BD) to isolate serum, which was stored at –80°C. Serum levels of troponin were determined by ELISA (Life Diagnostics Inc). Serum levels of amylase and lipase were determined by bioassay by the Washington University Division of Comparative Medicine core facility. Blood glucose was measured using an Ascensia Elite glucometer (Fisher) at a consistent time of the day to minimize diurnal variation.

IFN bioassay. IFN levels in the serum were determined by bioassay (60). Briefly, L929 cells were incubated for 24 hours with standards or samples, then infected with VSV-GFP for 10 hours. Cells were fixed and the percentage of GFP$^+$ cells as determined by flow cytometry was used to calculate IFN levels in the linear range of the standard curve. This method yielded results similar to those of an IFN-α ELISA (PBL; data not shown), but was more sensitive for low IFN values.

Histology. Organs were harvested at indicated time points after infection and tissue sections were prepared by either formalin-fixation paraffin embedding or freezing in OCT reagent. For morphology, multiple sections at different levels were stained for H&E. For immunohistochemistry, fixed tissue sections were stained using primary antibodies to the following antigens: EMCVpol (Ms, dilution 1:1500; provided by Ann Palmenberg, University of Wisconsin, Madison, Wisconsin, USA), CD3 (Rb mab, clone SP7, dilution 1:100; Thermo Scientific), MDA-5 (Helicard, mouse Rb polyclonal, dilution 1:600; Alexis Biochemicals), Iba-1 (Rb, dilution 1:500; Wako Chemicals), active caspase-3 (Rb, dilution 1:600; R&D), Synaptophysin (Rb mab, clone SP11, dilution 1:100; Thermo Scientific), and CD11c (hamster, clone HL3, dilution 1:10 overnight incubation; BD Biosciences — Pharmingen). Reactivity was revealed using EnVision HRP-linked Rb or Ms detection system (Dako) followed by diaminobenzidine (DAB) or using biotinylated goat anti-hamster secondary antibody (1:150; Vector Laboratories) followed by goat HRP-Polymer Kit (Biocare Medical) and DAB for CD11c staining. For double staining, after completing the first reaction, the second antibody was visualized using Mach 4 AP-linked Rb detection system (Biocare Medical) followed by Ferengi Blue (Biocare Medical). Anti-TLR3 staining (rat, clone 11F8.1B7, dilution 1:200; provided by David Segal, National Cancer Institute, Bethesda, Maryland, USA) was performed on 5-micron cryostat/frozen sections and developed using rabbit anti-rat IgG mouse Adsorbed biotinylated antibody (dilution 1:200; Vector Laboratories) followed by HRP streptavidin and DAB as chromogen. Anti-MDA5 staining was performed as previously described (51). Photomicrographs were obtained using the DP-70 Olympus digital camera mounted on the Olympus BX60 microscope.

Statistics. Statistical significance was calculated using 2-tailed Students *t* test for individual comparisons or log rank test for survival studies.

Acknowledgments

We would like to thank several colleagues for their generous donations of reagents: Richard Flavell and Lena Alexopolou for *Tlr3*$^{-/-}$ mice, Tadatsu Taniguchi for the *Irf3*$^{-/-}$ and *Ifnb*$^{-/-}$ mice, Ann Palmenberg for anti-EMCVpol antibody, David Segal (National Cancer Institute) for anti-TLR3 antibody, and John Corbett for EMCV-D virus stock. Suellen Greco of Washington University School of Medicine, Department of Comparative Medicine, provided assistance with the necropsies of infected animals. Speed congenics was performed by the Rheumatic Diseases core facility at Washington University. This project was supported by Juvenile Diabetes Research Foundation (JDRF) grant 24-2007-420 (to M. Colonna) and NIH grants DK058177 and P60DK20579 (to E.R. Unanue). S.A. McCartney was supported by National Research Service Award (NRSA) number F30HL096354 from the National Heart, Lung, and Blood Institute (NHLBI) and T32DK007296 from the National Institute of Diabetes and Digestive and Kidney Diseases (NIDDK). Cristina Rossini is supported by the Beretta Foundation (Brescia, Italy).

Received for publication June 14, 2010, and accepted in revised form January 19, 2011.

Address correspondence to: Marco Colonna, Washington University School of Medicine, Department of Pathology and Immunology, 425 S. Euclid Ave., Box 8118, St. Louis, Missouri 63110, USA. Phone: 314.362.0367; Fax: 314.362.4096; E-mail: mcolonna@pathology.wustl.edu.

1. Kawai T, Akira S. The role of pattern-recognition receptors in innate immunity: update on Toll-like receptors. *Nat Immunol*. 2010;11(5):373–384.
2. Wilkins C, Gale M Jr. Recognition of viruses by cytoplasmic sensors. *Curr Opin Immunol*. 2010; 22(1):41–47.
3. Pichlmair A, Reis e Sousa C. Innate recognition of viruses. *Immunity*. 2007;27(3):370–383.
4. Meylan E, Tschopp J, Karin M. Intracellular pattern recognition receptors in the host response. *Nature*. 2006;442(7098):39–44.
5. Yoneyama M, Fujita T. RNA recognition and signal transduction by RIG-I-like receptors. *Immunol Rev*. 2009;227(1):54–65.
6. Kato H, et al. Length-dependent recognition of double-stranded ribonucleic acids by retinoic acid-inducible gene-I and melanoma differentiation-associated gene 5. *J Exp Med*. 2008;205(7):1601–1610.
7. Takahasi K, et al. Solution structures of cytosolic RNA sensor MDA5 and LGP2 C-terminal domains: identification of the RNA recognition loop in RIG-I-like receptors. *J Biol Chem*. 2009;284(26):17465–17474.
8. Cui S, et al. The C-terminal regulatory domain is the RNA 5′-triphosphate sensor of RIG-I. *Mol Cell*. 2008;29(2):169–179.
9. Saito T, Owen DM, Jiang F, Marcotrigiano J, Gale M Jr. Innate immunity induced by composition-dependent RIG-I recognition of hepatitis C virus RNA. *Nature*. 2008;454(7203):523–527.
10. Satoh T, et al. LGP2 is a positive regulator of RIG-I- and MDA5-mediated antiviral responses. *Proc Natl Acad Sci U S A*. 2010;107(4):1512–1517.
11. Venkataraman T, et al. Loss of DExD/H box RNA helicase LGP2 manifests disparate antiviral responses. *J Immunol*. 2007;178(10):6444–6455.
12. Rothenfusser S, et al. The RNA helicase Lgp2 inhibits TLR-independent sensing of viral replication by retinoic acid-inducible gene-I. *J Immunol*. 2005;175(8):5260–5268.
13. Garcia-Sastre A, Biron CA. Type 1 interferons and the virus-host relationship: a lesson in detente. *Science*. 2006;312(5775):879–882.
14. Banchereau J, Pascual V. Type I interferon in systemic lupus erythematosus and other autoimmune diseases. *Immunity*. 2006;25(3):383–392.
15. Stetson DB, Medzhitov R. Type I interferons in host defense. *Immunity*. 2006;25(3):373–381.
16. Castano L, Eisenbarth GS. Type-I diabetes: a chronic autoimmune disease of human, mouse, and rat. *Annu Rev Immunol*. 1990;8:647–679.
17. Bach JF. Insulin-dependent diabetes mellitus as an autoimmune disease. *Endocr Rev*. 1994; 15(4):516–542.
18. Yoon JW, Austin M, Onodera T, Notkins AL. Isolation of a virus from the pancreas of a child with diabetic ketoacidosis. *N Engl J Med*. 1979;300(21):1173–1179.
19. Ginsberg-Fellner F, et al. Diabetes mellitus and autoimmunity in patients with the congenital rubella syndrome. *Rev Infect Dis*. 1985;7 suppl 1:S170–S176.
20. Andreoletti L, et al. Detection of coxsackie B virus RNA sequences in whole blood samples from adult patients at the onset of type I diabetes mellitus. *J Med Virol*. 1997;52(2):121–127.
21. Hyoty H, Taylor KW. The role of viruses in human diabetes. *Diabetologia*. 2002;45(10):1353–1361.
22. Ylipaasto P, et al. Enterovirus infection in human pancreatic islet cells, islet tropism in vivo and receptor involvement in cultured islet beta cells. *Diabetologia*. 2004;47(2):225–239.
23. Craighead JE, McLane MF. Diabetes mellitus: induction in mice by encephalomyocarditis virus. *Science*. 1968;162(856):913–914.
24. Guberski DL, et al. Induction of type I diabetes by Kilham's rat virus in diabetes-resistant BB/Wor rats. *Science*. 1991;254(5034):1010–1013.
25. Jun HS, Yoon JW. A new look at viruses in type 1 diabetes. *Diabetes Metab Res Rev*. 2003;19(1):8–31.
26. Oldstone MB, Nerenberg M, Southern P, Price J, Lewicki H. Virus infection triggers insulin-dependent diabetes mellitus in a transgenic model: role of anti-self (virus) immune response. *Cell*. 1991; 65(2):319–331.
27. Horwitz MS, Bradley LM, Harbertson J, Krahl T, Lee J, Sarvetnick N. Diabetes induced by Coxsackie virus: initiation by bystander damage and not molecular mimicry. *Nat Med*. 1998;4(7):781–785.
28. Horwitz MS, Ilic A, Fine C, Rodriguez E, Sarvetnick N. Presented antigen from damaged pancreatic beta cells activates autoreactive T cells in virus-mediated autoimmune diabetes. *J Clin Invest*. 2002;109(1):79–87.
29. von Herrath MG, Dockter J, Oldstone MB. How virus induces a rapid or slow onset insulin-dependent diabetes mellitus in a transgenic model. *Immunity*. 1994;1(3):231–242.
30. Devendra D, Eisenbarth GS. Interferon alpha--a potential link in the pathogenesis of viral-induced type 1 diabetes and autoimmunity. *Clin Immunol*. 2004;111(3):225–233.
31. Theofilopoulos AN, Baccala R, Beutler B, Kono DH. Type I interferons (alpha/beta) in immunity and autoimmunity. *Annu Rev Immunol*. 2005;23:307–336.
32. Li Q, Xu B, Michie SA, Rubins KH, Schreriber RD, McDevitt HO. Interferon-alpha initiates type 1 diabetes in nonobese diabetic mice. *Proc Natl Acad Sci U S A*. 2008;105(34):12439–12444.
33. von Herrath M. Can we learn from viruses how to prevent type 1 diabetes?: the role of viral infections in the pathogenesis of type 1 diabetes and the development of novel combination therapies. *Diabetes*. 2009;58(1):2–11.
34. Thomas VA, Woda BA, Handler ES, Greiner DL, Mordes JP, Rossini AA. Altered expression of diabetes in BB/Wor rats by exposure to viral pathogens. *Diabetes*. 1991;40(2):255–258.
35. Sobel DO, et al. Poly I:C induces development of diabetes mellitus in BB rat. *Diabetes*. 1992;41(4):515–520.
36. Huang X, Hultgren B, Dybdal N, Stewart TA. Islet expression of interferon-alpha precedes diabetes in both the BB rat and streptozotocin-treated mice. *Immunity*. 1994;1(6):469–478.
37. Moriyama H, et al. Induction and accelera-

tion of insulitis/diabetes in mice with a viral mimic (polyinosinic-polycytidylic acid) and an insulin self-peptide. *Proc Natl Acad Sci U S A*. 2002;99(8):5539–5544.
38. Wen L, Peng J, Li Z, Wong FS. The effect of innate immunity on autoimmune diabetes and the expression of Toll-like receptors on pancreatic islets. *J Immunol*. 2004;172(5):3173–3180.
39. Lang KS, et al. Toll-like receptor engagement converts T-cell autoreactivity into overt autoimmune disease. *Nat Med*. 2005;11(2):138–145.
40. Devendra D, et al. Interferon-alpha as a mediator of polyinosinic:polycytidylic acid-induced type 1 diabetes. *Diabetes*. 2005;54(9):2549–2556.
41. Smyth DJ, et al. A genome-wide association study of nonsynonymous SNPs identifies a type 1 diabetes locus in the interferon-induced helicase (IFIH1) region. *Nat Genet*. 2006;38(6):617–619.
42. Shigemoto T, Kageyama M, Hirai R, Zheng J, Yoneyama M, Fujita T. Identification of loss of function mutations in human genes encoding RIG-I and MDA5: implications for resistance to type I diabetes. *J Biol Chem*. 2009;284(20):13348–13354.
43. Nejentsev S, Walker N, Riches D, Egholm M, Todd JA. Rare variants of IFIH1, a gene implicated in antiviral responses, protect against type 1 diabetes. *Science*. 2009;324(5925):387–389.
44. von Herrath M. Diabetes: A virus-gene collaboration. *Nature*. 2009;459(7246):518–519.
45. Cerutis DR, Bruner RH, Thomas DC, Giron DJ. Tropism and histopathology of the D, B, K, and MM variants of encephalomyocarditis virus. *J Med Virol*. 1989;29(1):63–69.
46. Gaines KL, Kayes SG, Wilson GL. Altered pathogenesis in encephalomyocarditis virus (D variant)-infected diabetes-susceptible and resistant strains of mice. *Diabetologia*. 1986;29(5):313–320.
47. Kato H, et al. Differential roles of MDA5 and RIG-I helicases in the recognition of RNA viruses. *Nature*. 2006;441(7089):101–105.
48. Gitlin L, et al. Essential role of mda-5 in type I IFN responses to polyriboinosinic:polyribocytidylic acid and encephalomyocarditis picornavirus. *Proc Natl Acad Sci U S A*. 2006;103(22):8459–8464.
49. Hardarson HS, et al. Toll–like receptor 3 is an essential component of the innate stress response in virus–induced cardiac injury. *Am J Physiol Heart Circ Physiol*. 2007;292(1):H251–H258.
50. Bar-On L, Jung S. Defining dendritic cells by conditional and constitutive cell ablation. *Immunol Rev*. 2010;234(1):76–89.
51. McCartney S, et al. Distinct and complementary functions of MDA5 and TLR3 in poly(I:C)-mediated activation of mouse NK cells. *J Exp Med*. 2009;206(13):2967–2976.
52. Edwards AD, et al. Toll-like receptor expression in murine DC subsets: lack of TLR7 expression by CD8 alpha+ DC correlates with unresponsiveness to imidazoquinolines. *Eur J Immunol*. 2003; 33(4):827–833.
53. Van Rooijen N. The liposome-mediated macrophage 'suicide' technique. *J Immunol Methods*. 1989; 124(1):1–6.
54. Louten J, van Rooijen N, Biron CA. Type 1 IFN deficiency in the absence of normal splenic architecture during lymphocytic choriomeningitis virus infection. *J Immunol*. 2006;177(5):3266–3272.
55. Honda K, Takaoka A, Taniguchi T. Type I interferon [corrected] gene induction by the interferon regulatory factor family of transcription factors. *Immunity*. 2006;25(3):349–360.
56. Dotta F, et al. Coxsackie B4 virus infection of beta cells and natural killer cell insulitis in recent-onset type 1 diabetic patients. *Proc Natl Acad Sci U S A*. 2007;104(12):5115–5120.
57. Casanova JL, Abel L, Quintana-Murci L. Human TLRs and IL-1Rs in host defense: natural insights from evolutionary, epidemiological, and clinical genetics [published online ahead of print October 26, 2010]. *Annu Rev Immunol*. doi:10.1146/annurev-immunol-030409-101335.
58. Jung S, et al. In vivo depletion of CD11c+ dendritic cells abrogates priming of CD8+ T cells by exogenous cell-associated antigens. *Immunity*. 2002;17(2):211–220.
59. Sato S, et al. Toll/IL-1 receptor domain-containing adaptor inducing IFN-beta (TRIF) associates with TNF receptor-associated factor 6 and TANK-binding kinase 1, and activates two distinct transcription factors, NF-kappa B and IFN-regulatory factor-3, in the Toll-like receptor signaling. *J Immunol*. 2003;171(8):4304–4310.
60. Takaoka A, et al. Cross talk between interferon-gamma and -alpha/beta signaling components in caveolar membrane domains. *Science*. 2000;288(5475):2357–2360.